UC Santa Barbara

UC Santa Barbara Previously Published Works

Title

Collective Rayleigh-Plateau Instability: A Mimic of Droplet Breakup in High Internal Phase Emulsion

Permalink

https://escholarship.org/uc/item/0zk9d27x

Journal

Langmuir, 32(11)

ISSN

0743-7463

Authors

Mansard, Vincent
Mecca, Jodi M
Dermody, Dan L
et al.

Publication Date

2016-03-22

DOI

10.1021/acs.langmuir.5b04727

Peer reviewed

eScholarship.org Powered by the California Digital Library
University of California

LANGMUIR

Article

pubs.acs.org/Langmuir

Collective Rayleigh-Plateau Instability: A Mimic of Droplet Breakup in High Internal Phase Emulsion

Vincent Mansard,[†] Jodi M. Mecca,[‡] Dan L. Dermody,[‡] David Malotky,[‡] Chris J. Tucker,[‡] and Todd M. Squires*[,†]

[†]Department of Chemical Engineering, University of California, Santa Barbara, California 93106-5080, United States

[‡]Formulation Science, Core Research and Development, The Dow Chemical Company, Midland, Michigan 48674, United States

Supporting Information

ABSTRACT: Using a microfluidic multi-inlet coflow system, we show the Rayleigh-Plateau instability of adjacent, closely spaced fluid threads to be collective. Although droplet size distributions and breakup frequencies are unaffected by cooperativity when fluid threads are identical, breakup frequencies and wavelengths between mismatched fluid threads become locked due to this collective instability. Locking narrows the size distribution of drops that are produced from dissimilar threads, and thus the polydispersity of the emulsion. These observations motivate a hypothesized two-step mechanism for high internal phase emulsification, wherein coarse emulsion drops are elongated into close-packed fluid threads, which break into smaller droplets via a collective Rayleigh Plateau instability. Our results suggest that these elongated fluid threads break cooperatively, whereupon wavelength-locking reduces the ultimate droplet polydispersity of high-internal phase emulsions, consistent with experimental observations.

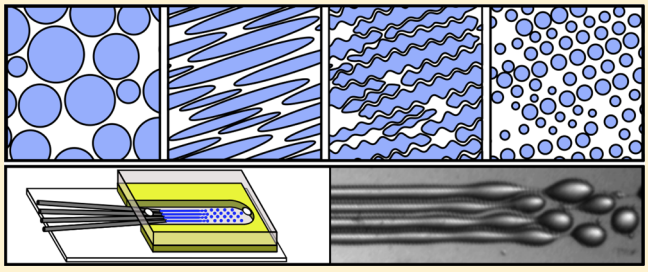

INTRODUCTION

An emulsion is a dispersion of drops of one fluid in another immiscible fluid[1] that enables the compatibilization of insoluble active components. They improve product performance, reduce production costs, and enable new applications. Emulsions find use in a wide variety of industrial processes, including food, personal care, cleaning products, pharmaceuticals, agrochemicals, coatings, inks, mining, and oil recovery.[1,2]

Controlling drop size distribution remains a challenge of major industrial significance, as it affects emulsion stability, rheology, and targeted performance.[3] The size dispersion depends strongly on the emulsification process. Numerous emulsification processes exist, and can be classified into mechanical[4,5] and nonmechanical processes.[4,6] Unfortunately, processes with tight control over drop size have low throughput, and are inadequate for industrial production. Large-scale emulsification typically involves strong, crude shearing processes to achieve the needed throughput, but produce emulsions with high polydispersity ($\gtrsim$100%).[7]

Fundamental understanding of emulsification under shear has been limited primarily to the breakup of isolated droplets in laminar flow.[8] Three main behaviors have been identified, depending on the shear history. When flow rates are slowly increased, droplets split into two primary droplets and several satellite droplets.[9] In this case, droplet breakup is controlled by the capillary number $\mathrm{Ca} = \eta\dot{\gamma}r/\sigma$, where η is the viscosity, σ the surface tension, $\dot{\gamma}$ the shear rate, and r the drop radius. Under suddenly imposed strong flows, by contrast, droplets form long threads that break into multiple droplets[10,11] via Rayleigh-Plateau instability (RPI).[12] This regime is going to be the most relevant in the framework of this article. Other breakup processes also occur, particularly under certain surfactant conditions- for example, tipstreaming occurs when flows convect surfactant toward stagnation point on drop surfaces, where it concentrates and facilitates the formation and ejection of tiny droplets.[13]

Mechanisms by which high dispersed-phase mixtures are emulsified are much less understood, given the interactions between drops. Direct visualization of emulsification is difficult, with only limited observations thus far,[14,15] and relations are essentially empirical. Drop size distributions for moderate internal phase fractions ($\phi \lesssim 70\%$) have been successfully described using models for isolated drop breakup, and simply replacing the continuous phase viscosity with the overall emulsion viscosity to account for the drop interactions.[14,16,17] Nevertheless, no simple model exists to describe emulsification at higher volume fraction.[14,18]

Surprisingly low polydispersity has been observed for emulsions produced with high internal phase concentrations and strong shear rates.[19,20] These observations complement the work of Bibette and colleagues,[15,21] who produced very low-polydispersity emulsions (~20%) by shearing a crude premixed emulsion at homogeneous stress within a thin-gap Couette cell, with sufficiently concentrated crude emulsions or sufficiently shear-thinning continuous phase. A two-step mechanism was

Received: December 28, 2015
Revised: February 24, 2016

 © XXXX American Chemical Society

DOI: 10.1021/acs.langmuir.5b04727
Langmuir XXXX, XXX, XXX−XXX

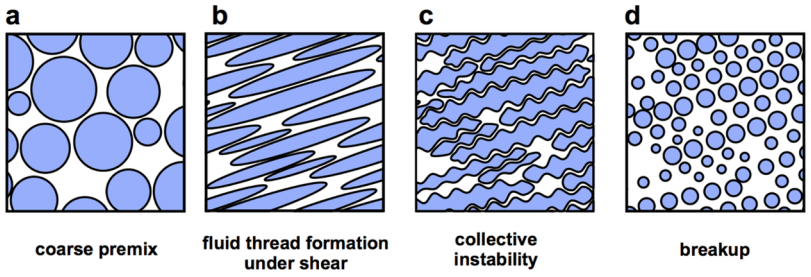

Figure 1. Hypothesized mechanism for high-internal phase emulsification. (a) Polydisperse drops of a coarse premix under high shear to form elongated fluids threads (b), which break due to a collective Rayleigh-Plateau instability (c) to form smaller droplets (d), whose polydispersity is reduced due the collective nature of the instability.

proposed to describe emulsification within this system,[15] wherein the strong, homogeneous shear deforms the dispersed phase into long, thin threads with homogeneous diameters, that subsequently break into homogeneous droplets (Figure 1).

In this Article, we focus on the RPI of adjacent fluid threads (Figure 1c,d). We demonstrate that this RPI-driven breakup is cooperative in nature, and that the collective breakup of arrays of close fluid threads reduces the polydispersity of the resulting emulsion. We suggest that the two-step mechanism of Bibette and co-workers holds for more general mixing geometries: coarse emulsion drops in high-internal phase mixtures are deformed to form closely packed arrays of long fluid threads, which eventually break up into droplets via an RPI that is necessarily collective. Indeed, collective instabilities have been observed experimentally and numerically.[22−25]

This work focuses on the second step of this mechanism: how the collective RPI of concentrated arrays of threads impacts the characteristics of the droplets that form. Our experiments reveal clear cooperativity among adjacent threads as they break, yet a surprising lack of impact on the size of the drops that form among arrays of homogeneous threads. Threads of different radii also break in a cooperative fashion, which acts to produce droplets that are closer in size than would be produced were such threads to have broken into drops in isolation. This phenomenon reduces the polydispersity of emulsions produced in our devices, and suggests a mechanism for polydispersity reduction in the emulsification of high internal phase fraction mixtures.

MATERIALS AND METHODS

To study the collective effects in the RPI experimentally, we have developed a microfluidic multi-inlet coflow system. Oil is flowed through the main channel, and either oil or water is flowed through each of the adjacent capillaries to produce between one and four independently controllable aqueous threads (Figure 2b−d). The single-thread configuration corresponds to the previous literature,[26−28] whereas two- and four-thread configurations are used to vary thread interactions and study their impact on collective instability and droplet formation. All experiments reported here are conducted in the so-called jet regime at high flow rates, where breakup occurs far from capillary inlets[27,28] via the RPI.[28]

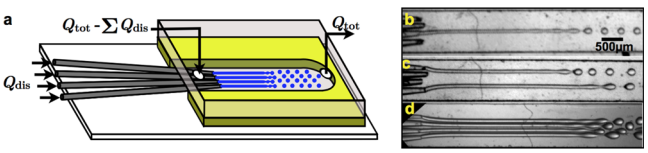

Figure 2. (a) Microfluidic chip capable of producing up to four aqueous fluid threads, coflowing within an (immiscible) silicon oil stream. Configurations with (b) one, (c) two, and (d) four aqueous threads can be produced simply by flowing either continuous or dispersed phase fluid through each capillary inlet, as desired.

Coflow is realized using four circular glass capillaries (VitroTubes) as nozzles that inject the dispersed phase into continuous phase fluid flowing through a rectangular, 400 μm × 1.5 mm × 4 cm channel (Figure 2a), with four polydimethylsiloxane (PDMS) walls. Channels are made within a 400 μm-thick layer of PDMS on top of a glass slide coated with a thin PDMS layer. Choosing capillaries with 330 ± 30 μm OD ensures the output threads are nearly centered within the 400 μm-tall PDMS channel. Thinner threads are produced by using a micropipette puller to taper the capillary diameter down to 150 μm. Once capillaries have been positioned and secured, the top of the device is covered with a thick PDMS block. All junctions between PDMS layers are strengthened by ozone-bonding and cured at 120 °C overnight.

The model system consists of silicon oil (Sigma-Aldrich 100 cP) with 200 mPa·s viscosity (measured with TA AR-G2 rheometer) as the continuous phase, and 60%$_w$ sucrose solutions (180 mPa.s viscosity) as the dispersed phase. 1%$_w$ TTAB surfactant is added to the dispersed phase to decrease surface tension, and to stabilize drops and threads against coalescence.

Thread diameters D_t before the instability are controlled by the ratio Q_{dis}/Q_{tot}, where Q_{tot} and Q_{dis} are the total flow rate and the dispersed phase flow rate through one nozzle, respectively.[28] If the channel aspect ratio is large ($w/h \gg 1$), thread diameters are small ($D_t/h \ll 1$), and phases are viscosity-matched, then thread diameters are given by

$$D_t = \sqrt{\frac{8wh(1 - 0.63h/w)}{3\pi}}\sqrt{\frac{Q_{dis}}{Q_{tot}}} \quad (1)$$

where w and h are the channel width and the height, respectively (see Supporting Information (SI)).

HOMOGENEOUS THREAD DIAMETERS

In the jet regime, breakup is not perfectly periodic, but the position where breakups occur fluctuates. We manually detect the positions of the thread tips (where breakup has occurred) (Figure 3), with a precision of 30 μm (3 pixels), in each frame. Despite the fast instability period (0.1 s between breakup events), the positions of the thread tips exhibit slower fluctuations, over few-second time scales. In the closed-packed four-thread configuration, slow fluctuations of distinct threads are clearly correlated, whereas well-separated threads are not (Figure 3c,d).

To confirm this observation, we calculate the correlation coefficient

$$C = \frac{\langle \Delta p_i . \Delta p_{i+1} \rangle}{\sqrt{\langle \Delta p_i^2 \rangle \langle \Delta p_{i+1}^2 \rangle}} \quad (2)$$

where p_i is the tip position of thread i, and $\Delta p_i = p_i - \langle p_i \rangle$. For the two-thread configuration (Figure 3a,c), the correlation coefficient $C = 0.2 \pm 0.1$, indicating no significant correlation. The

DOI: 10.1021/acs.langmuir.5b04727
Langmuir XXXX, XXX, XXX−XXX

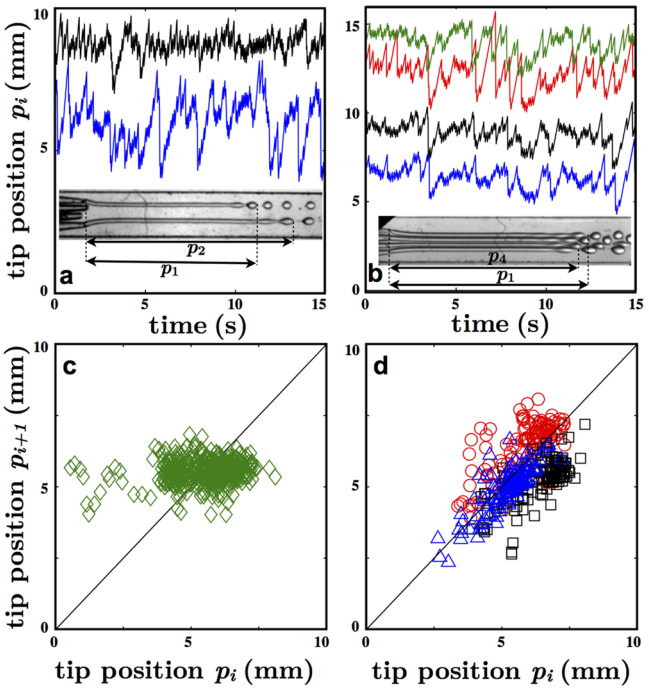

Figure 3. (a,b) Distance of each thread tip p_i from the capillary inlet vs time (thread positions are shifted by 3 mm for clarity) . (c,d) Tip positions p_{i+1} as a function of the tip positions p_i of the adjacent threads when breakup occurs - the black lines correspond to $y = x$. We observe significant correlation between breakup events in the four-thread system (b and d), but little to no correlation for the two-thread system (a and c) . Data acquired for Q_{dis} = 10 μL/min and D_t = 138 μm. In (d), the symbols ○, □, and △ correspond to the top, middle top, and middle bottom threads as a function of the middle top, middle bottom, and bottom threads, respectively.

RPI becomes a collective, cooperative process when multiple fluidic threads are close and interact hydrodynamically (Figure 3b,d). The correlation coefficients for all pairs of adjacent threads range between C = 0.65 and 0.75, next-nearest-neighboring threads have lower correlation coefficient (C = 0.50 and 0.60), and outermost threads show less correlation (C = 0.4) (Table S1).

Surprisingly, the collective nature of the RPI had no measurable impact on the size of droplets produced from equal-sized threads. Each breakup event gives rise to a main droplet (~140 μm radius) and a satellite droplet (~30 μm) . The droplet radius distribution is measured by analyzing the microscopy images in Matlab using the watershed algorithm[29] (Figure 4a, inset). Distributions for both configurations are nearly identical (Figure 4a), with a well-defined primary peak, suggesting that cooperativity between breaking threads does not change droplet size. We compute a volume-averaged polydispersity P, as is standard for emulsions,[4] which is found to be P = 10 ± 0.5% for both two- and four-thread experiments (SI). Satellite drops have a negligible impact on the polydispersity (ΔP ~ 0.5%).

Consistent results hold over a range of flow rates, in both the one-thread (control) and the four-thread (collective) configurations. Specifically, the dispersed phase flow rate Q_{dis} is increased in 1 μL/min steps while keeping the flow rate ratio Q_{dis}/Q_{tot} constant, in order to keep the thread diameter D_t constant. After each change in Q_{dis}, flows are allowed to stabilize for 2 min. The breakup frequency ν_b is measured for each system computing the temporal power spectrum for 1000 images, and extracting the dominant frequency with a Gaussian fit (SI). Breakup frequencies for both configurations are found to be identical. Mass conservation dictates that the mean drop volume V_d be related to Q_{dis} via

$$V_d = Q_{dis}/\nu_b \quad (3)$$

RPI cooperativity does not affect the breakup frequency ν_b and therefore does not impact the drop size.

Moverover, Figure 4b reveals a linear relationship $\nu_b = A(D_t)$ Q_{dis} between the breakup frequency ν_b and Q_{dis}, wherein the proportionality constant $A(D_t)$ depends on the thread diameter, irrespective of the number of threads. The mean droplet volume $V_d = 1/A(D_t)$ thus depends exclusively on the thread diameter D_t, as does the mean droplet radius $R_d = (3/4\pi A(D_t))^{1/3}$. Finally, the drop radius is found to grow linearly with thread diameter, via $R_d = (1.09 \pm 0.04)D_t$ [Figure 5c], consistent with previous measurements on isolated threads.[30] In our experiments, instability wavelengths λ are constrained by volume conservation to obey

$$V_d = \pi D_t^2 \lambda/4 \quad (4)$$

which here implies that $\lambda = (6.9 \pm 0.8)D_t$, in good agreement with the classical RPI where the most unstable wavelength also varies linearly with D_t.[12]

We have shown significant cooperativity in the RPI breakup of identical, closely spaced fluid threads; however, this collective instability does not affect the drop size distribution. On one hand, this is sensible: isolated threads break with a given wavelength, and multiple threads can break with this wavelength in a coordinated fashion. Cooperative effects simply template the breakup of closely packed, identical threads. On the other hand, these observations seem at odds with the reduced polydispersity attained in high internal phase emulsification, where cooperative breakup is expected. When coarse premixtures are subjected to spatiotemporally inhomogeneous mixing flows, however, significant polydispersity in thread diameters should be expected. After all, drop polydispersity attained using even isolated coflowing threads (P ~ 10%) is significantly lower than in conventionally produced emulsions ($P \gtrsim$ 100%).

INHOMOGENEOUS THREAD DIAMETERS

We therefore study cooperativity in the breakup of threads that are closely spaced, yet *inhomogeneous* in diameter. In this case, we show that collective effects can "lock" the breakup frequency and wavelength of adjacent but mismatched threads, thereby reducing differences between drop diameters, and ultimately polydispersity.

To create threads with different diameters, we control the dispersed phase flow rate Q_{dis} through each nozzle individually, operating in both the two-thread (low interaction) or four-thread (high interaction) configurations [Figure 5, insets], and measure the breakup characteristics as described above. All but one of the threads is created with a particular diameter D_0, which is held constant for each set of experiments by maintaining Q_{dis} through these nozzles and Q_{tot} constant. The diameter D_1 of the mismatched thread is initially created with D_1 ~ $0.1D_0$, and increased to D_1 ~ $1.2D_0$ in steps of 1 μL/min. Once the system has stabilized after each change in Q_1, the breakup frequency ν_b is measured for each thread, by calculating the power spectra from 1000 subimages of each thread (100 × 2-pixel subimages, centered on the thread axis).

DOI: 10.1021/acs.langmuir.5b04727
Langmuir XXXX, XXX, XXX−XXX

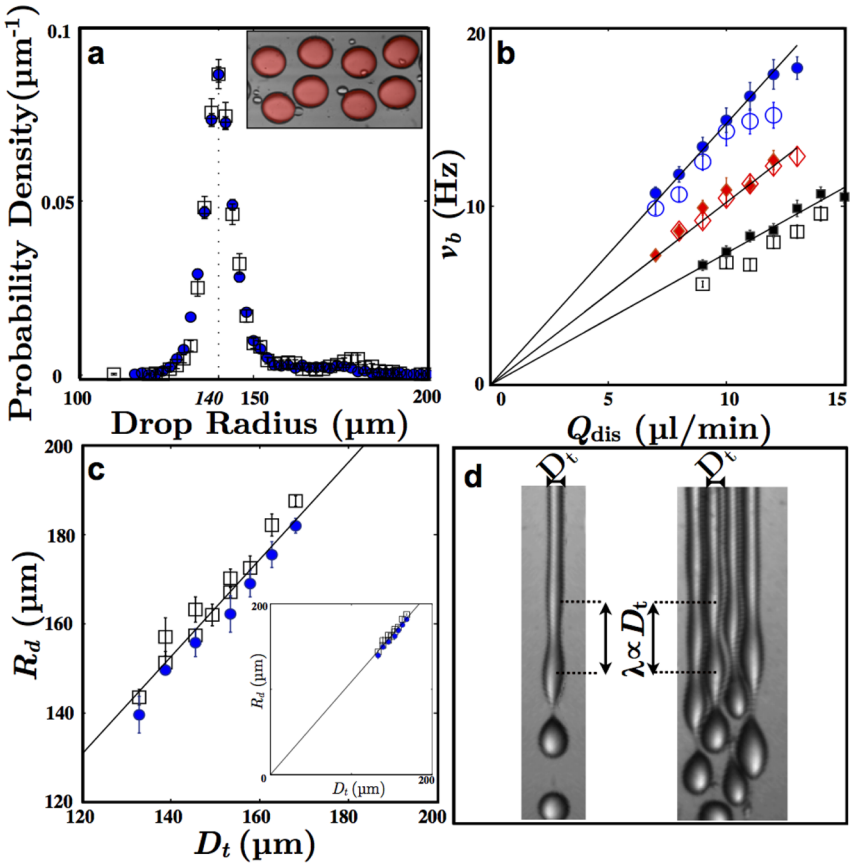

Figure 4. (a) Drop radius distributions in (□) 4-thread and (●) 2-thread configurations, for Q_{dis} = 10 μL/min and D_t = 138 μm. (Inset) A typical micrograph, with detected drops colored red. (b) Breakup frequency ν_b vs Q_{dis}, with thread diameter D_t held fixed at (□,■) 163 μm, (◊,♦) 146 μm, (○,●) 133 μm. No significant difference is seen between cooperative (four-thread, open symbols) and free (one-thread, filled symbols). (c) Mean drop radii R_d calculated using ν_b for (□) 4-thread and (●) 1-thread configurations, vary linearly with thread diameter D_t via $R_d = (0.97 \pm 0.03)D_t$. (d) Typical instability for one- and four-thread configurations reveal the breakup wavelength $\lambda \propto D_t$, unaffected by thread interactions.

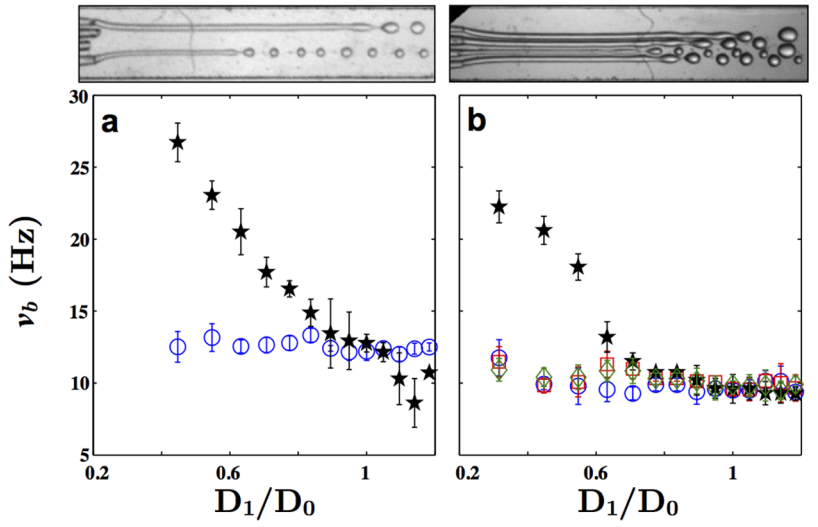

Figure 5. Breakup frequencies measured for individual threads with mismatched diameters with D_0 = 138 μm and $Q_{dis,0}$ = 10 μL/min. Threads with fixed thread diameter D_0 are shown as (○,□,◇) and mismatched diameter D_1 (★) are shown for (a) two-thread and (b) four-thread configuration. Notably, breakup frequencies are locked over a wide range of D_1/D_0 when breakup is cooperative (four-thread), compared with the free (two-thread) configuration.

Cooperativity has a dramatic impact on the breakup frequency of the mismatched thread D_1. Two breakup regimes are evident, depending on the strength of interactions between threads. Droplets form noncooperatively in the two-thread system, where threads are far enough apart that hydrodynamic interactions are too weak (Figure 5a), and in the four-thread configuration when the threads are too heterogeneous (Figure 5b, e.g., $D_1 \lesssim 0.5D_0$). Mismatched threads break cooperatively, however, when thread

DOI: 10.1021/acs.langmuir.5b04727
Langmuir XXXX, XXX, XXX−XXX

diameters are close enough (Figure 5b, when, e.g., $D_1 \gtrsim 0.7D_0$). In this case, the breakup frequency ν_1 of the mismatched thread is locked to the dominant frequency ν_0 of the neighboring threads.

Further evidence for the relationship between cooperativity and frequency-lock is shown in Figure 6, which shows the correlation coefficient C for the tip positions of the two central threads as a function of (mismatched) thread diameter D_1. In the four-thread configuration, we observe two different regimes: for $D_1 < 0.7D_0$, $|C| < 0.2$, indicating no cooperativity in the breakup, whereas for $D_1 = 0.7D_0$ or closer, the correlation index shows a qualitative jump to $C \approx 0.5-0.7$, indicating much stronger cooperativity. Notably, this cooperativity transition corresponds directly to the frequency-locking transition. In the two-thread configuration, we measure $|C| < 0.2$ for all diameter ratios, indicating no cooperation, as expected.

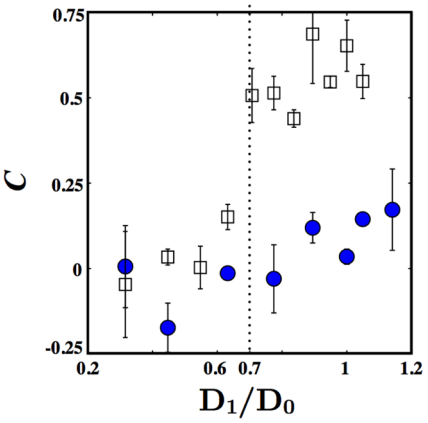

Figure 6. Correlation coefficient C (eq 2) between the tip positions of the mismatched thread and of its adjacent one in (□) four-thread and (●) 2-thread configurations (Figure 5a,b). High values of C are observed in the four-thread configuration for $D_1 \gtrsim 0.7D_0$, indicating cooperative breakup and frequency lock are observed for the same conditions.

Frequency-locking in the breakup of mismatched threads implies wavelength-locking as well. Combining eq 3 with eq 4 gives $\lambda_i = 4Q_i/\pi\nu_i D_i^2$, and since $Q_i \propto D_i^2$ via eq 1, we find that $\lambda_1 = \lambda_0$ when $\nu_1 = \nu_0$ in the frequency-locked regime. This wavelength lock is directly evident from visual inspection (Figure 7a).

Drop radii are proportional to thread diameter $R_1 \propto D_1$ in the free breakup regime, but not in the collective regime. Indeed, volume conservation requires $V_1 \propto \lambda D_1^2$ (eq 4). In the collective breakup regime, the mismatched thread wavelength is "locked" to the dominant wavelength, meaning $\lambda \propto D_0$ rather than D_1. Drops formed from "mismatched" threads should thus have radii

$$\frac{R_1}{R_0} = \begin{cases} D_1/D_0 & \text{free RPI} \\ (D_1/D_0)^{2/3} & \text{collaborative RPI} \end{cases} \quad (5a,b)$$

These two scaling relations, which have no adjustable parameters, agree quantitatively with measured drop radii (Figure 7b).

Equations 5a,b and Figure 7b show that collectivity in the breakup of inhomogeneous threads reduces the range of droplet sizes that are produced, and naturally suggests a mechanism for the reduction of polydispersity in high-internal phase emulsification. A collection of threads whose diameters have relative standard deviation $\Delta D/D$ would break into drops with radius distribution $R_d \propto D_t$ under conditions of free breakup, implying droplet radii have the same dispersion $\Delta R/R = \Delta D/D$ as the initial threads. Under conditions where breakup is cooperative, however, wavelength-locking produces droplets with radii $R_d \propto D_t^{2/3}$, giving $\Delta R/R \sim (2/3)\,\Delta D/D$ in the $\Delta D \ll D$ limit, for a 30% reduction.

DISCUSSION AND OUTLOOK

This work has focused specifically on cooperatively in the Rayleigh-Plateau instability of adjacent fluid cylinders. We have shown that breakup happens to be collective when threads are sufficiently closely packed. It is also important to distinguish this source of collective effects from another types of confinement that would be due to the presence of rigid walls. In the experiments reported here, thread surfaces remain sufficiently separated ($\gtrsim$10 μm) during the growth of the cooperative instability that hydrodynamic interactions play the dominant role, as had been assumed in previous computational studies.[22,24] Nonhydrodynamic interactions (e.g., electrostatic, steric, or disjoining forces) may become significant in systems where threads are spaced much more closely, and should be considered in such systems.

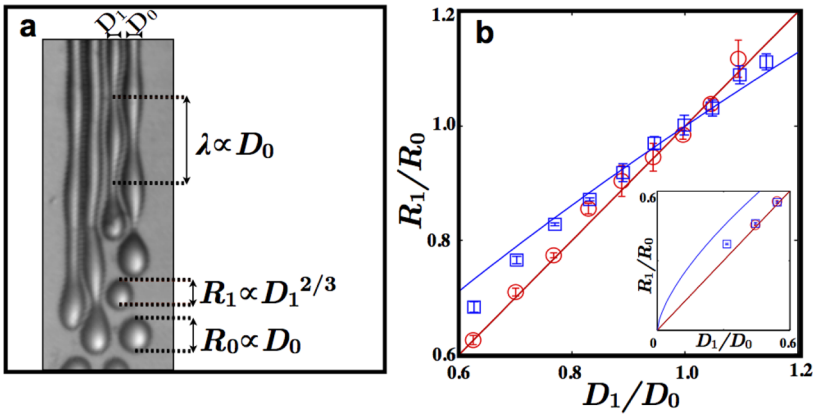

Figure 7. (a) Collective instability with one mismatched thread ($D_1/D_0 = 0.7$). Breakup wavelengths λ are equal, even though thread diameters are not. (b) Reduced drop size R_1/R_0 vs reduced thread diameter D_1/D_0 for two-thread (○) and four-thread (□) configurations. When breakup is locked (four-thread, with $D_1/D_0 \gtrsim 0.7$), "mismatched" drop radii follow eq 5a (blue line), whereas nonlocked threads (i.e., two-thread, or four-thread with $D_1/D_0 \lesssim 0.5$) follow eq 5b (red line).

DOI: 10.1021/acs.langmuir.5b04727
Langmuir XXXX, XXX, XXX−XXX

Surprisingly, close-packed arrays of identical threads break at the same frequency (and therefore wavelength) as they would if isolated. Cooperative instabilities have a profound impact on mismatched threads; however, over a broad range of 'mismatched' radius ratios, breakup frequencies and wavelengths become 'locked' at the dominant wavelength established by the array. Significantly, this locking renders the drop sizes produced by mismatched fluid threads to be less polydisperse than if those same threads broke up in isolation.

This study was motivated more broadly by reports of low polydispersity in high internal-phase emulsification. While we have not directly interrogated the HIPE formation process itself, we propose that wavelength-locking in the collective RPI provides a natural mechanism for low-polydispersity HIPE formation via a two-step emulsification process. Our experiments were designed specifically to probe one aspect of high-internal-phase emulsification, and to identify and elucidate processes that may contribute to polydispersity reduction. When (and whether) the cooperative RPI mechanism we have identified here plays a role in more complex emulsification processes is left for future study.

Specifically, there are at least two sources of polydispersity in emulsification of the sort described here: (1) variability among the drop radii that form a particular thread of given diameter (i.e., spread about the mean diameter), and (2) variability of the initial threads themselves (i.e., variance in the mean drop diameters). Our results reveal that collective effects do not affect the first source: the variance about the mean droplet diameter from each thread appears unaffected by cooperativity. The effect that cooperative breakup does have, by contrast, is in reducing the impact of polydispersity among the original threads. The frequency- (or wavelength)-locking between threads of unequal radii gives rise to mean drop radii that are much closer in size than would have occurred without the cooperativity. Scaling arguments, and experimental results, suggest up to 30% reduction in the polydispersity of mean droplet radii produced from dissimilar threads. The extent to which this mechanism plays a role in 'practical' high-internal phase emulsification will depend on many factors, including whether polydispersity is dominated by the variance among the drops produced by each thread, or by the variance among the thread radii.

Even more broadly, the mechanism we have demonstrated here, and which we have hypothesized as plausible for more complex systems, requires that concentrated pre-emulsions stretch when stirred to form close-packed arrays of fluid cylinders before breaking. Whether this occurs depends upon many factors, including viscosity ratio, internal phase fraction, and interfacial tension. We expect these conditions to be met at large Ca (so that viscous stresses deform drops much more rapidly than capillary stresses), and when the continuous phase viscosity matches that of the dispersed phase, so that the multiphase blend initially deforms affinely with the mixing flow to form close-packed thread arrays. These effects, which are important to elucidate, are left for future work.

■ ASSOCIATED CONTENT

Supporting Information

The Supporting Information is available free of charge on the ACS Publications website at DOI: 10.1021/acs.langmuir.5b04727.

Details on the relation between flow rates and thread diameter, on the correlation coefficient C, on the definition on the polydispersity P, and on the method to measure ν_b (PDF)

Video of experiments (AVI)

■ AUTHOR INFORMATION

Corresponding Author

*E-mail: squires@engineering.ucsb.edu.

Notes

The authors declare no competing financial interest.

■ ACKNOWLEDGMENTS

Support from the Dow Chemical Company thru the materials Institute at UCSB is gratefully acknowledged.

■ REFERENCES

(1) Heusch, R. *Ullmann's Encyclopedia of Industrial Chemistry*; Wiley-VCH: Weinheim, Germany, 2000.

(2) Schramm, L. L., Ed. *Emulsions: Fundamentals and Applications in the Petroleum Industry*; Advances in Chemistry Series; American Chemical Society: Washington, DC, 1992; Vol. *231*.

(3) Barnes, H. a. Rheology of emulsions - a review. *Colloids Surf., A* **1994**, *91*, 89−95.

(4) Leal-Calderon, F.; Schmitt, V.; Bibette, J. *Emulsion Science: Basic Principles*; Springer: New York, 2007.

(5) Simons, J. M. M.; Keurentjes, J. T. F.; Meuldijk, J. Micron-sized polymer particles by membrane emulsification. *Macromol. Symp.* **2013**, *333*, 102−112.

(6) Perazzo, a.; Preziosi, V.; Guido, S. Phase inversion emulsification: Current understanding and applications. *Adv. Colloid Interface Sci.* **2015**, *222*, 581−599.

(7) Calabrese, R. V.; Wang, C. Y.; Bryner, N. P. Drop breakup in turbulent stirred-tank contactors. Part III: Correlations for mean size and drop size distribution. *AIChE J.* **1986**, *32*, 677−681.

(8) Stone, H. Dynamics of drop deformation and breakup in viscous fluids. *Annu. Rev. Fluid Mech.* **1994**, *26*, 65−102.

(9) Bentley, B. J.; Leal, L. G. An experimental investigation of drop deformation and breakup in steady, two-dimensional linear flows. *J. Fluid Mech.* **1986**, *167*, 241.

(10) Mikami, T.; Cox, R.; Mason, S. Breakup of extending liquid threads. *Int. J. Multiphase Flow* **1975**, *2*, 113−138.

(11) Taylor, G. I. The Formation of Emulsions in Definable Fields of Flow. *Proc. R. Soc. London, Ser. A* **1934**, *146*, 501−523.

(12) Tomotika, S. On the Instability of a Cylindrical Thread of a Viscous Liquid Surrounded by Another Viscous Fluid. *Proc. R. Soc. London, Ser. A* **1935**, *150*, 322.

(13) Eggleton, C.; Tsai, T.-M.; Stebe, K. Tip Streaming from a Drop in the Presence of Surfactants. *Phys. Rev. Lett.* **2001**, *87*, 048302.

(14) Golemanov, K.; Tcholakova, S.; Denkov, N.; Ananthapadmanabhan, K.; Lips, a. Breakup of bubbles and drops in steadily sheared foams and concentrated emulsions. *Phys. Rev. E* **2008**, *78*, 051405.

(15) Mabille, C.; Leal-Calderon, F.; Bibette, J.; Schmitt, V. Monodisperse fragmentation in emulsions: Mechanisms and kinetics. *Europhys. Lett.* **2003**, *61*, 708−714.

(16) Loewenberg, M.; Hinch, E. J. Numerical simulation of a concentrated emulsion in shear flow. *J. Fluid Mech.* **1996**, *321*, 395.

(17) Jansen, K. M. B.; Agterof, W. G. M.; Mellema, J. Droplet breakup in concentrated emulsions. *J. Rheol.* **2001**, *45*, 227.

(18) Vankova, N.; Tcholakova, S.; Denkov, N. D.; Ivanov, I. B.; Vulchev, V. D.; Danner, T. Emulsification in turbulent flow 1. Mean and maximum drop diameters in inertial and viscous regimes. *J. Colloid Interface Sci.* **2007**, *312*, 363−80.

(19) Welch, C.; Rose, G.; Malotky, D.; Eckersley, S. Rheology of high internal phase emulsions. *Langmuir* **2006**, *22*, 1544−1550.

(20) Tcholakova, S.; Lesov, I.; Golemanov, K.; Denkov, N. D.; Judat, S.; Engel, R.; Danner, T. Efficient emulsification of viscous oils at high drop volume fraction. *Langmuir* **2011**, *27*, 14783−96.

DOI: 10.1021/acs.langmuir.5b04727
Langmuir XXXX, XXX, XXX−XXX

(21) Mason, T. G.; Bibette, J. Emulsification in viscoelastic media. *Phys. Rev. Lett.* **1996**, *77*, 3481−3484.
(22) Hagedorn, J.; Martys, N.; Douglas, J. Breakup of a fluid thread in a confined geometry: droplet-plug transition, perturbation sensitivity, and kinetic stabilization with confinement. *Phys. Rev. E* **2004**, *69*, 056312.
(23) Elemans, P. H. M.; van Wunnik, J. M.; van Dam, R. a. Development of morphology in blends of immiscible polymers. *AIChE J.* **1997**, *43*, 1649−1651.
(24) Knops, Y. M. M.; Slot, J. J. M.; Elemans, P. H. M.; Bulters, M. J. H. Simultaneous breakup of multiple viscous threads surrounded by viscous liquid. *AIChE J.* **2001**, *47*, 1740−1745.
(25) Janssen, P. J. A.; Meijer, H. E. H.; Anderson, P. D. Stability and breakup of confined threads. *Phys. Fluids* **2012**, *24*, 012102.
(26) Eggers, J.; Villermaux, E. Physics of liquid jets. *Rep. Prog. Phys.* **2008**, *71*, 036601.
(27) Utada, A. S.; Fernandez-Nieves, A.; Stone, H. a.; Weitz, D. a. Dripping to jetting transitions in coflowing liquid streams. *Phys. Rev. Lett.* **2007**, *99*, 094502.
(28) Guillot, P.; Colin, A.; Utada, A.; Ajdari, A. Stability of a Jet in Confined Pressure-Driven Biphasic Flows at Low Reynolds Numbers. *Phys. Rev. Lett.* **2007**, *99*, 104502.
(29) Vincent, L.; Soille, P. Watersheds in digital spaces: an efficient algorithm based on immersion simulations. *IEEE Transactions on Pattern Analysis and Machine Intelligence* **1991**, *13*, 583−598.
(30) Cubaud, T.; Mason, T. G. Capillary threads and viscous droplets in square microchannels. *Phys. Fluids* **2008**, *20*, 053302.

DOI: 10.1021/acs.langmuir.5b04727
Langmuir XXXX, XXX, XXX−XXX